Computers & Security 113 (2022) 102571

Contents lists available at ScienceDirect

Computers & Security

journal homepage: www.elsevier.com/locate/cose

TC 11 Briefing Papers

Open-Set source camera identification based on envelope of data clustering optimization (EDCO)

Bo Wang, Yue Wang*, Jiayao Hou, Yi Li, Yanqing Guo

Dalian University of Technology, No.2 Linggong Road, Ganjingzi District, Dalian, China

ARTICLE INFO

Article history:
Received 17 August 2021
Revised 19 November 2021
Accepted 30 November 2021
Available online 3 December 2021

Keywords:
Source camera identification
Open-Set recognition
Digital image forensics
Image processing
Multimedia security

ABSTRACT

The task of source camera identification is devoted to linking an image to the source camera model and plays a significant role in forensics. Nevertheless, with the ongoing development of new camera models, it is difficult to keep a model database up to date, giving rise to the open-set problem. To deal with this problem, we propose a novel approach based on the envelope of data clustering optimization (EDCO). The new EDCO scheme can identify the camera model regardless of whether or not it is included in the database. The experimental results prove that EDCO efficiently separates unknown source images from known source images and links the query image identified as known with the source camera model. When the dataset is expanded with the new camera model, EDCO only needs to train the new model instead of retraining with all models together, which greatly improves the scalability. Compared with the state of the art, our method can effectively distinguish between images from known and unknown camera models, even in extreme cases.

© 2021 Elsevier Ltd. All rights reserved.

1. Introduction

In the era of digital image ubiquity, determining how to accurately identify the source of a digital image has become a hot topic in the field of information security (González and Woods, 1981). Source camera identification plays an important role in improving the security of digital images, resolving copyright disputes, preventing false publicity and combating cyber crimes, especially, it can provide favourable technical support for judicial authentication and criminal investigations such as child pornography and insurance claims (Li, 2010).

For conventional closed-set source camera identification approaches (Ahmed et al., 2019; Bayram et al., 2005; Kang et al., 2012; Li et al., 2018; Yang et al., 2019), the test image is usually generated by a known model (included in our dataset). However, new models are joining market rapidly (Schweighofer et al., 2008), and it is challenging to keep the dataset up to date. Since source camera identification is basically a classification problem (Choi et al., 2006; Freire-Obregón et al., 2019; Lekshmi and Vaithiyanathan, 2018; Zheng et al., 2020), lack of new models in an out-of-date dataset may cause mis-classification; that is, the images captured by new models are classified as some old model. Therefore, identifying unknown image sources has become one of the most critical challenges in current source camera identification (Bayar and Stamm, 2018).

The consideration of open-set issues in the field of camera source identification can be first traced back to 2009 Wang et al. (2009), a source camera identification method based on the combination of OC-SVM (one-class support vector machine) and MC-SVM (multi-class support vector machine) was proposed, which considered the camera model problem of unknown sources for the first time. Although Huang et al. (2015) distinguish between known and unknown models, the recognition accuracy of known models is very low when there are few known models. In this paper, we propose a novel approach based on the envelope of data clustering optimization (EDCO). For our EDCO scheme, we recharacterize the classification boundary of the data by clustering, effectively solving the problem of low recall rates in the case when there are few known models. Mayer et al. (2020); Mayer and Stamm (2018) address similar issues but with a much more limited scope. The authors can only determine the "siblingship" between two input images, that is, whether the two images originate from the same source camera model. Additionally, their methods require a relatively large training set and lack efficacy. When the test images are captured by models including unknown models, our EDCO scheme effectively distinguishes the known images from the unknown images and determines which model the known image belongs to.

* Corresponding author.
E-mail addresses: bowang@dlut.edu.cn (B. Wang), 31909072@mail.dlut.edu.cn (Y. Wang), 769724342@qq.com (J. Hou), liyi@dlut.edu.cn (Y. Li), guoyq@dlut.edu.cn (Y. Guo).

https://doi.org/10.1016/j.cose.2021.102571
0167-4048/© 2021 Elsevier Ltd. All rights reserved.

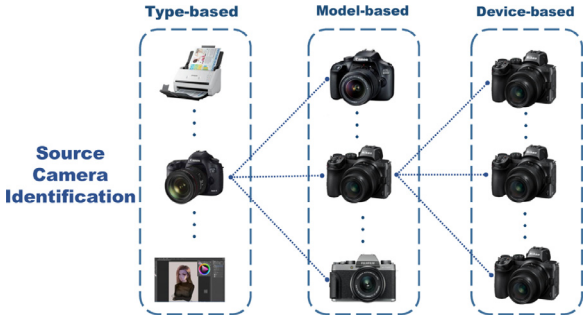

Fig. 1. Three levels of identification granularity.

The key contributions of this paper are as follows:

- We propose the EDCO scheme to address the open-set problem of source camera identification, which can effectively distinguish between the images from known and unknown camera models.
- To overcome the problem of the low recall rate of known camera models in bad situation (there is quantity gap between known models and unknown models), the EDCO scheme describes the distribution boundary of a camera model in the feature space in a more detailed manner based on the envelope of data clustering optimization.
- When the dataset is expanded with the new camera model, EDCO only needs to train the new model instead of retraining with all models in the training set together, which is more scalable on the "future" camera models and overcomes the time-consuming problem in the era of rapid development of camera models.
- We prove the effectiveness of the EDCO scheme through a large number of experiments. The obtained results demonstrate that the proposed EDCO scheme significantly outperforms the state-of-the-art methods in terms of model extensibility and robustness.

The rest of the paper is organized as follows. Section 2 formally introduces the representative studies related to our work. Section 3 describes our proposed method in detail. Comprehensive experiments are carried out and comparisons of related works are presented in Section 4 to verify the superiority of the proposed method. Finally, we conclude the paper in Section 5.

2. Related work

In this section, we briefly introduce the traditional closed-set source camera identification and the open-set problem.

2.1. Source camera identification

As a challenging branch of the digital forensics domain, source camera identification aims to determine the original sources of digital images. On the one hand, depending on the different cases and the available reference information, source camera identification may be approached at three levels (Wang et al., 2009) of identification granularity, as illustrated in Fig. 1.

1. Type-based: electronic scanner, digital camera, computer generated, etc.;
2. Model-based: Canon_Ixus55, Nikon_D70, Fuji_J50, etc.;
3. Device-based: Nikon_D70_1, Nikon_D70_2, Nikon_D70_3, etc.

On the other hand, source camera identification can generally be divided into two groups by different forensics points: active source camera identification and blind source camera identification. This work is a **model-based** approach and focuses on blind

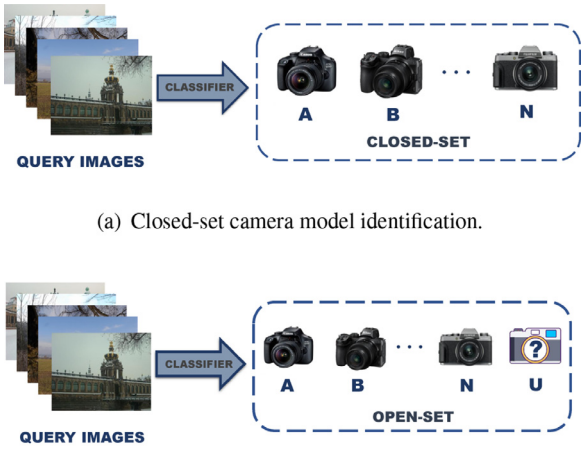

(a) Closed-set camera model identification.

(b) Open-set camera model identification.

Fig. 2. Different camera model identification problem formulations.

source camera identification, which does not need to embed the source information.

Since different camera manufacturers and even different camera models from the same manufacturer may have various colour filter array configuration algorithms and colour transformations, Kharrazi et al. (2004) propose a total of 34 features to capture the differences in the underlying colour characteristics for different camera models. Bayram et al. (2005) believe that the images captured by digital cameras are greatly affected by the colour filter array (CFA) and demosaicing algorithms. The authors propose a method based on a proprietary interpolation algorithm trajectory to identify the source camera model. A unified grey-level invariant local binary pattern (LBP) is used to capture features or artefacts generated by the image processing algorithm implemented inside the camera in Xu and Shi (2012). Recent work in digital image forensics suggests that convolutional neural networks (CNNs) (Bayar and Stamm, 2017; Bondi et al., 2017a; Rafi et al., 2020; Tuama et al., 2016) can be used to learn the camera's features. Huang et al. (2018) design a new image source identification scheme which can capture both the feature coupling and model coupling relationships. Liu et al. (2019) propose a new Anti-noise Image Source Identification (AISI) method to deal with noisy samples of image source identification. In addition, the problem of limited labels classification is also an important problem in source camera identification. Sameer and Naskar (2020) use a few shot learning technique known as deep siamese network to address the problem of performing accurate source camera identification, with a limited set of labelled training samples, per camera model.

2.2. Camera model identification in the open set

When a traditional forensic method is used to link an image to the source camera model, images from an unknown model may be misclassified into a known camera model in the closed-set, as depicted in Fig. 2(a). For an open-set camera model identification as shown in Fig. 2(b), the classifier is permitted to reject an image from an unknown model instead of distributing an incorrect label from the known dataset randomly.

Few works have addressed the problem of unknown models in source camera identification. Wang et al. (2009) propose a combined classification framework of the one-class SVM and the multi-class SVM. The one-class SVM is trained for each model to determine whether an image is from the known model. If an image does not belong to any known model, it will be rejected as an unknown model. In contrast, the accepted images will be input into the

multi-class SVM employed to determine which known model this image is from. Costa et al. (2012, 2014) propose a method based on decision boundary sculpting (DBC). The method first considers the images of known models as positive samples and considers images of other known models as negative samples. Then, by adjusting the decision boundary to minimize false positive matches in the future, the binary SVM is trained to distinguish between positive samples and negative samples. Due to the lack of information about unknown models, the decision boundary of DBC may not be well shaped in actual situations. Huang et al. (2015) propose the source camera identification with unknown models (SCIU) scheme to address the open-set problem. The authors first use a KNN-based unknown detection method to identify some sample images of unknown models from the unlabelled training dataset. Then, they employ a self-training procedure to extract more sample images of unknown models from the unlabelled training dataset. As a result of the algorithm characteristics of KNN, the prediction accuracy of the known model is low when the sample is unbalanced, and the computational complexity and spatial complexity are also high.

With the rapid progress in computer graphics and computer vision, in 2017, Bondi et al. (2017b) demonstrated the possibility of using CNNs in camera model identification for the first time. Bayer and Stamm Bayar and Stamm (2018) propose a thresholding protocol over the maximum confidence score to identify unknown cameras. They first use a constrained CNN to extract camera model identification features and then map the learned deep features onto confidence scores to indicate whether the two image patches are captured by the same or different camera models. If the confidence score is lower than the thresholding, the query image will be identified as unknown. Mayer and Stamm (2018) propose a system to compare the source camera model of two image patches, even when the camera models are unknown to the investigator. First, the authors train a CNN-based feature extractor to output general and advanced features, encoding the source camera model information of the image patch. In addition, they learn a similarity measure that maps these feature pairs to the scores associated with each known camera model. Finally, the score is used as a criterion for judging whether two images belong to the same source camera model. However, the authors can only determine the "siblingship" between two input images to identify whether they originate from the same camera model or not. Additionally, their methods require a relatively large training set and are inefficient (as this method can only test the relationship between two images at a time instead of classifying all images in the test set). In Júnior et al. (2019), the authors formalize and evaluate open-set training protocols applied to open-set classification methods during training for proper estimate of parameters for the open-set scenario and carry out large-scale testing on the open-set camera model identification problem considering independent datasets and several algorithms. In Mayer et al. (2020), Mayer et al. design a video-specific camera model verification system comprising a deep feature extractor, similarity network, and video-level fusion system. Based on the similarity network, the method can classify whether the two query videos were captured by the same camera model.

3. Proposed approach

In this section, we propose a machine learning model named Envelope of Data Clustering Optimization(EDCO) for unknown model detection in source camera identification. There are two main operational steps in the proposed model: (i) Model training with positive samples and (ii) Unknown model separation and known model linking. Fig. 3 shows the overall workflow of the proposed method. The implementation process is described in detail in the following subsections.

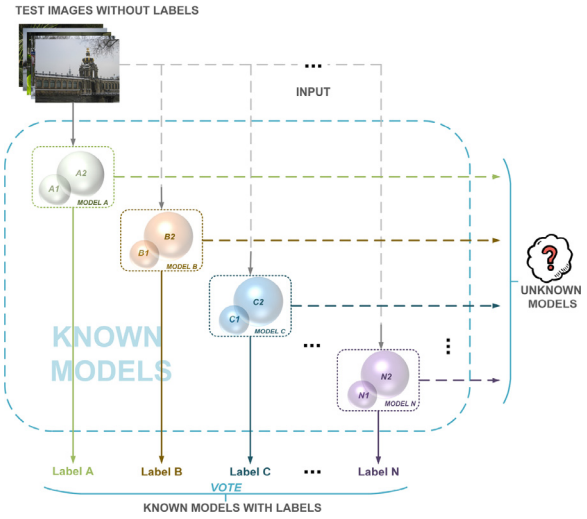

Fig. 3. The workflow of Envelope of Data Clustering Optimization(EDCO). Each small dotted box represents a known camera model from the training set, which is an envelope formed by the fusion of several hyperspheres. By combining all the small dotted boxes in the training set, the EDCO scheme can be obtained. If the test image is rejected by all hypersurface envelopes, it will be judged as an unknown source image (as shown in the dotted line); if the image is accepted by more than one hypersurface envelope (as shown in the solid line), it will need to be voted on to determine which camera is the known source.

3.1. Model training with positive samples

The first step in our approach is to train models with positive samples (images from one known source camera model), such that it allows the classifier to identify the samples associated with unknown models during testing.

As a new single-class classifier, support vector data description (SVDD)Liu et al. (2012); Tax and Duin (2004) simulates the boundary of target data through the minimum volume hypersphere and has been widely used in anomaly detection. However, the distribution of the samples in the eigenspace is often complex and unpredictable, and SVDD in some cases does not perform well in describing the boundaries of positive samples, particularly when the distinction between classes is not large in the high-dimensional feature space. Therefore, our algorithm proposes to divide the samples in each camera model by clustering.

Fig. 4 introduces the basic principle of the algorithm in a simple schematic where the red bounding lines represent misclassified samples. A sample distribution in the feature space is given as shown in Fig. 4(a). As depicted in Fig. 4(b), some positive samples may be misclassified into negative classes when the hypersurface radius is too small. However, when the hypersurface radius is too large, the negative samples from the unknown models will be wrongly identified as the positive samples, as shown in Fig. 4(c). Therefore, to enable the model to accept the positive samples from the known camera model to the maximum extent while rejecting the negative samples from the unknown camera models, our Algorithm 1 focuses on the refinement of the positive envelope in the feature space. As shown in Fig. 4(d), the original samples are divided into $\mathcal{K}$ separate subsets by the clustering method (Fig. 4(d) shows the case of $\mathcal{K}$), and the hypersurface envelope of each sample is described. In this case, the number of misclassified samples will decrease with envelope optimization.

The detailed training process is described below. First, given a labelled training dataset $\mathcal{T}_R$ with N classes (subsets), each class $\Gamma(\eta)$ is associated with a camera model indexed by η. That is, $\Gamma(\eta) \subset \mathcal{T}_R, \forall \eta \in (1, 2, \ldots, N)$ and η stands for the label of each camera model. Next, the colour filter array (CFA) (Bayram et al.,

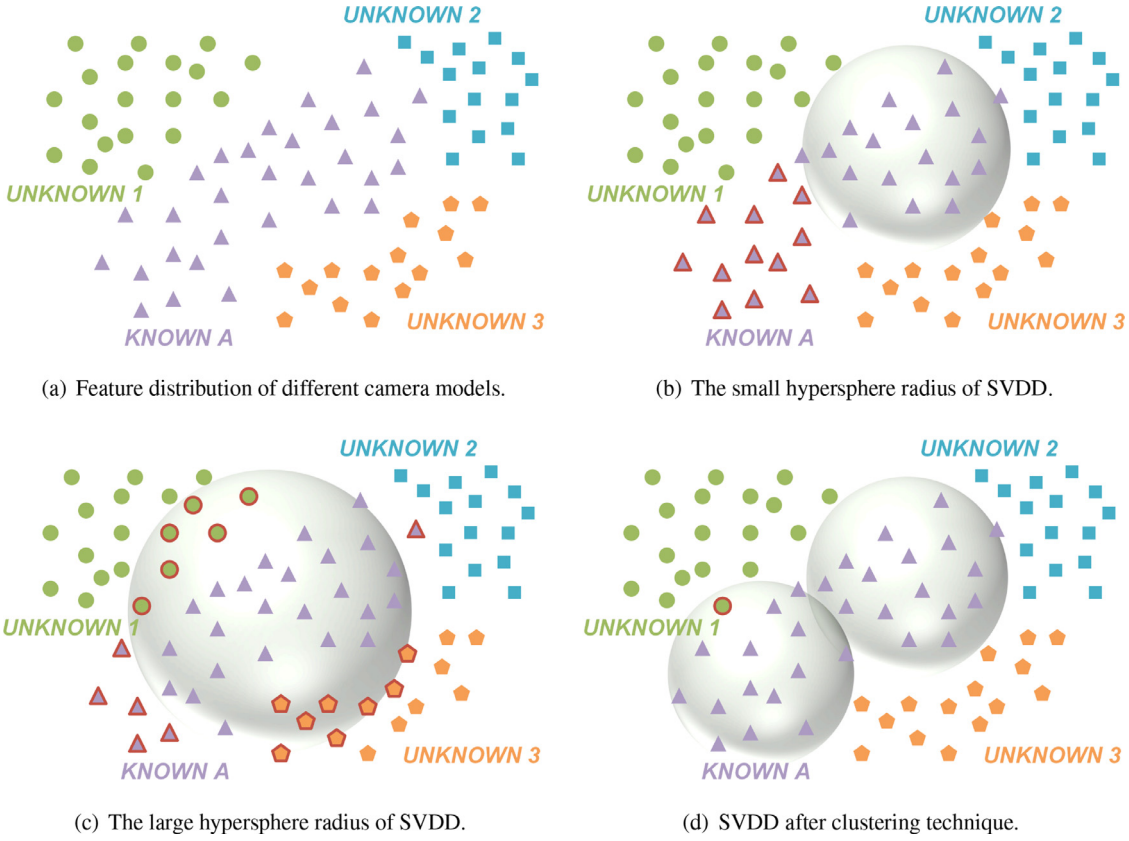

(a) Feature distribution of different camera models.

(b) The small hypersphere radius of SVDD.

(c) The large hypersphere radius of SVDD.

(d) SVDD after clustering technique.

Fig. 4. Analysis of problems in the training of positive samples. Purple triangles represent positive samples (known camera model), and graphics with other colours represent negative samples (unknown camera models).

Algorithm 1: Model Training with Positive Samples.

Input: Taining images: $x_i^{\eta_k}, i = 1, 2, \ldots, n$
The number of subclasses: $\mathcal{K}$
Output: Hypersphere models

Initialize centres: Randomly selected
Initialize Iteration = 0
while *1* **do**
  for *each* $x_i^{\eta_k}$ **do**
    Euclidean distance($x_i^{\eta_k}$,centres)
    Assign $x_i^{\eta_k}$ to the closest subclass
  New centres: Update centres using the sample mean of each subclass
  if *New centres* ! = *centres* **then**
    Iteration ← Iteration+1
    centres = New centres
    Repeat
  else
    Stop Iteration
    Break and **return** $\mathcal{K}$ subclasses
for *each subclass* **do**
  The formula 1–4
return K hypersphere models

2005) is used to extract features from the images in the training set; this is a widely used interpolation algorithm in source camera identification. By applying CFA interpolation, we obtain the 480-dimensional features (Wang et al., 2018) of images from N classes in $\mathcal{T}_R$. Then, in the 480-dimension feature space, $\mathcal{K}$-means (García et al., 2018) clustering is carried out for the positive samples, as described in detail in Algorithm 1.

For each class $\Gamma(\eta)$, we divide the data into $\mathcal{K}$ subclasses by applying clustering techniques and name each subclass as $\gamma(\eta_k)$, where η_k is a virtual label assigned to $\gamma(\eta_k)$ and distinguished by subscripts k. That is, $\gamma(\eta_k) \subset \Gamma(\eta), \forall k \in (1, 2, \ldots, K)$. Then,for each subclass $\gamma(\eta_k)$, the technique of SVDD is applied. Suppose each image is represented by $x_i^{\eta_k}$, where n is the number of positive samples (images) in $\gamma(\eta_k)$. That is, $x_i^{\eta_k} \in \gamma(\eta_k), \forall i \in (1, 2, \ldots, n)$. Suppose $x_i^{\eta_k}$ satisfies the nonlinear transformation Φ: $x_i^{\eta_k} \to F$. Therefore, SVDD can be described by the following optimization problem:

$$\begin{aligned} &displaystyle \min_{\mathbf{a},R,\xi} R^2 + C\sum_i \xi_i, \\ &displaystyle \text{ s.t. } \left\| \Phi(x_i^{\eta_k}) - \mathrm{a} \right\|^2 \le R^2 + \xi_i, \xi_i \ge 0, \end{aligned} \tag{1}$$

where a is the centre and R is the radius of the hypersphere (the formula will be shown later in Eq. 3). ξ_i is the relaxation factor and C represents a penalty parameter that balances the volume and error fraction of the hypersphere. By introducing Lagrangian multipliers by Liu et al. (2012); Tax and Duin (2004), the original problem can be transformed into a dual problem:

$$\begin{aligned} &displaystyle \min_{\alpha_i} \sum_{i=1}^{n}\sum_{j=1}^{n} \alpha_i\alpha_j K\left(\mathrm{x}_i^{\eta_k}, \mathrm{x}_j^{\eta_k}\right) - \sum_{i=1}^{n} \alpha_i K\left(\mathrm{x}_i^{\eta_k}, \mathrm{x}_i^{\eta_k}\right), \\ &displaystyle \text{ s.t. } \quad 0 \le \alpha_i \le C, \sum_{i=1}^{n} \alpha_i = 1, \end{aligned} \tag{2}$$

where α_i is the Lagrangian coefficient for $x_i^{\eta_k}$. $K\left(x_i^{\eta_k}, x_i^{\eta_k}\right)$ is the kernel function, which is equivalent to the inner product of the eigenspace. The corresponding Lagrangian coefficients of all samples can be obtained by solving the dual problem. In all training

samples, the samples for which the Lagrangian coefficients satisfy $0 \le \alpha_i \le C$ are called support vectors. It is assumed that the sample set composed of support vectors in the training dataset is **V**. By taking advantage of the kernel function, the boundaries mapped to the input space are no longer limited to spherical distributions. The centre and radius of a hypersphere are formulated as follows:

$$\mathrm{a}_{\eta_k} = \sum_{i=1}^{n} \alpha_i \Phi(x_i^{\eta_k}), \tag{3}$$

$$R_{\eta_k} = \left[K\left(x_v^{\eta_k}, x_v^{\eta_k}\right) - 2\sum_{i=1}^{n} \alpha_i K\left(x_v^{\eta_k}, x_i^{\eta_k}\right) + \sum_{i=1}^{n}\sum_{j=1}^{n} \alpha_i \alpha_j K\left(x_i^{\eta_k}, x_j^{\eta_k}\right) \right]^{\frac{1}{2}}, \tag{4}$$

where $x_i^{\eta_k} \in \mathbf{V}$. The data description of the positive training samples can be obtained by the centre and radius of the hypersphere.

To summarize, the proposed EDCO can effectively reject the unknown samples even if the training set has only one known camera model (extreme cases). Compared to other existing methods, our EDCO is more scalable on the "future" camera models; that is, once the dataset needs to add some new camera models, it is only necessary to train for each new camera model instead of retraining all the known camera models in the dataset.

3.2. Unknown model separation and known model linking

For the second step, we aim to (i) identify and separate images from known/unknown source models and (ii) link the images from the known models to the matched models.

First, for the test images, the following is given: an unlabelled test dataset $\mathcal{T}_E$ that contains images from known and unknown camera models, hypersphere models M_{η_k} that are obtained from Algorithm 1, and η_k as the label of one known source camera model in the training dataset. Next, the CFA interpolation algorithm (Wang et al., 2018) is used to extract features from the images in $\mathcal{T}_E$. According to SVDD Liu et al. (2012); Tax and Duin (2004), for each hypersphere, the distance from x_{test} to the centre of the hypersphere is:

$$d_{\eta_k} = \left[K(x_{\text{test}}, x_{\text{test}}) - 2\sum_{i=1}^{n} \alpha_i K\left(x_{\text{test}}, x_i^{\eta_k}\right) + \sum_{i=1}^{n}\sum_{j=1}^{n} \alpha_i \alpha_j K\left(x_i^{\eta_k}, x_j^{\eta_k}\right) \right]^{\frac{1}{2}}. \tag{5}$$

According to the formula 4, if $d_{\eta_k} \le R_{\eta_k}$ (the test sample is on the hypersphere or inside of the hypersphere), it will be judged as a normal sample from the known camera model; otherwise, it will be judged as a sample from the unknown camera models. Continuing with Algorithm 1, we define:

$$\hat{d_{\eta_k}} = d_{\eta_k} / R_{\eta_k}, \tag{6}$$

and we obtain the following decision rules:

1. For all hypersphere models M_{η_k} that are generated by Algorithm 1, if all the $\hat{d_{\eta_k}}$ rest content with $\hat{d_{\eta_k}} > 1$, we believe that the test image is from an unknown camera model outside our dataset. Then, we place the test image into the set of unknown source ($\mathcal{S}_u$).
2. If any $\hat{d_{\eta_k}} \le 1$, the test image is judged to belong to the set of known source ($\mathcal{S}_k$). Next, we vote on images in $\mathcal{S}_k$ to determine their corresponding camera models.
3. If the test image is accepted by only one hypersphere or some hyperspheres from the same camera model (hyperspheres with the same real label η but belonging to different subclasses, including η_1, η_2, η_3, etc.), we believe that it belongs to the class corresponding to the hypersphere.
4. If the test image is accepted by more than one hypersphere from different camera models (hyperspheres with different real labels η), it will be assigned to the class that has the most acceptant hyperspheres with the same real label η. If the number of accepting hyperspheres with the same real label η is the same, we will select the hypersphere where $min(\hat{d_{\eta_k}})$ is and assign the label to the test image.

By applying the distance judgement rule, we can classify images from $\mathcal{S}_k$ and associate the query image identified as known with the source camera model.

4. Experiments and results

In this section, we conduct extensive experiments to evaluate the proposed method on the source camera model identification on an open set. The detailed experimental setup and experimental results are described below.

4.1. Settings

In this paper, we use the Dresden image dataset (Gloe and Böhme, 2010), whose images are captured by different indoor/outdoor cameras with various camera settings; this dataset is considered a benchmark dataset for source camera identification and provides almost 17,000 images from 74 cameras ranging across 27 different models.

To eliminate the influence of different individuals of the same camera model, the samples in the training, validation and test sets of the same camera model are from different individuals. In our experiments, we first randomly select 100 images from each camera model in the Dresden image dataset and collect them as the test samples. Then, the rest of the images that we do not select in the first step will be divided into the training set and validation set at a 7:3 ratio. The detailed information about the camera models is shown in Table 1. Compared with the case in which the samples in the training and test set are all from the same individual of each camera model, this approach for dataset division is more difficult but can ensure that the used samples are mutually exclusive.

In our experiments, we extract CFA features (Wang et al., 2018) on all samples because a number of previous studies have reported that this method is effective and has been widely used in traditional forensic methods (Alattar et al., 2015; Gao et al., 2012; Liu et al., 2018). Because the image size of the 27 camera models is different, we extract the CFA from the 256× 256 subimage cropped from the centre. We conduct all our experiments in MATLAB on a CPU with 8 processors and 8 GB RAM.

Our proposed EDCO method is compared with the following source camera model identification methods on the open set in the experiments:

1. Combined classification framework prior to applying data clustering (CCF_B) (Wang et al., 2009);
2. Source camera identification with unknown models (SCIU) (Huang et al., 2015);
3. Mayer et al. similarity (Mayer et al., 2020; Mayer and Stamm, 2018);

In order to illustrate the effectiveness of the proposed algorithm in data clustering preprocessing, two self-comparison experiments are also set in this paper:

Table 1
Camera models used in the experiments.

No.	Camera Model	Abbr.	Number
1	Kodak_M1063	K1	2391
2	Olympus_mju1050SW	O1	1040
3	Praktica_DCZ5.9	PR1	1019
4	Panasonic_DMCFZ50	PA1	931
5	Casio_EXZ150	CA1	925
6	Nikon_CoolPixS710	N1	925
7	Ricoh_GX100	R1	854
8	Nikon_D200	N2	752
9	Sony_DSCT77	SO1	725
10	Samsung_L74wide	S1	686
11	Samsung_NV15	S2	645
12	Pentax_OptioA40	P1	638
13	FujiFilm_FinePixJ50	F1	630
14	Rollei_RCP7325XS	RO1	589
15	Canon_Ixus70	C1	567
16	Sony_DSCH50	SO2	541
17	Sony_DSCW170	SO3	405
18	Agfa_Sensor530s	A1	372
19	Nikon_D70	N3	369
20	Nikon_D70s	N4	367
21	Agfa_DC830i	A2	363
22	Agfa_DC733s	A3	281
23	Canon_Ixus55	C2	224
24	Pentax_OptioW60	P2	192
25	Canon_PowerShotA640	C3	188
26	Agfa_Sensor505x	A4	172
27	Agfa_DC504	A5	169

1. CCF_A: First, use the clustering algorithm to cluster the camera models of each original category into $\mathcal{K}$ subcategories, and then applied Combined classification framework(CCF_B) (Wang et al., 2009) to gets the decision model;
2. EDCO_B: Instead of using data clustering preprocessing to subdivide the camera models, the decision models are constructed by using hypersphere envelope according to the features of each camera model.

All the above methods are implemented for the Dresden image database. In addition, CCF_B and EDCO_B are compared in the experiments to demonstrate the effectiveness of the first algorithm in our proposed EDCO method.

4.2. Evaluation metrics

To evaluate the performance of the proposed EDCO method, we use the following metrics (Huang et al., 2015):

1. The known camera model accuracy (KACC) is the ratio of the number of the correctly identified images in the known camera models to the total number of images from the known camera models and is used to evaluate the ability of our proposed EDCO method to recall the known source images. Specifically, we define the number of correctly identified known source images as NCK and the number of the images identified from known models as NK.

$$\mathrm{KACC} = \mathrm{NCK}/\mathrm{NK} \tag{7}$$

2. The unknown camera model accuracy (UACC) is the ratio of the number of correctly identified images in the unknown camera models to the total number of images from the unknown camera models and reflects the ability of known - unknown separation of our proposed EDCO method. Specifically, we define the number of correctly identified unknown source images as NCU and the number of images identified from unknown models as NU.

$$\mathrm{UACC} = \mathrm{NCU}/\mathrm{NU} \tag{8}$$

Table 2
Overall accuracy (%) performance comparison of the approach.

Methods \Metrics	KACC	UACC	OACC
CCF_A	54.2	92.6	91.3
CCF_B	50.7	89.8	88.4
SCIU	28.9	96.5	94.4
EDCO_B	69.5	96.3	95.3
EDCO	**83.6**	**96.7**	**96.2**

3. The overall camera model accuracy (OACC) is the ratio of the total number of correctly identified images to the total number of images and is used to measure the overall identification accuracy.

$$\mathrm{OACC} = \frac{\text{No. of correctly identified images}}{\text{No. of all images identified}} \tag{9}$$

4.3. Results and discussion

4.3.1. Study of EDCO

Experiment I: To test and evaluate our proposed method, we design experiments based on the Dresden dataset as follows. Each time, we pick a model from dataset (which is treated as the "known" model) for training our classifier. Then, we use the remaining 26 other models in the dataset as "unknown" models. The KACC, UACC, and OACC values obtained using EDCO and other methods are given in Figs. 5–7 for comparison.

An examination of the experiment results presented in Fig. 5 shows that EDCO is significantly superior to the other methods. The EDCO_B method is the second best, with an average accuracy rate 18.0% lower than that of EDCO. The SCIU method has the worst stability and the lowest accuracy on average, as reflected by the fact that the KACC of the SCIU method can reach 100.0% when K1 is used as the known source camera model, while the KACC of the SCIU method reaches only 8.0% when A4 is used as the known source camera model. The performance of the CCF_A method is generally better than that of the CCF_B method. Similarly, the EDCO method is also superior to the EDCO_B method, which is attributed to the application of Algorithm 1 that describes the hypersurface envelope in more detail. However, CCF_B and EDCO_B need to exclude the possible influence of the camera model from unknown sources, so the hypersurface envelope radius should be as small as possible, resulting in the drawback of a relatively low KACC. Generally, the EDCO method has a strong recall capability for the known source camera models, with an average KACC of 83.6%. The KACC values of all methods are very low on N4 and N5 because these two models of cameras have negligible differences in brand and hardware structure. Therefore, some scholars regard them as the same model in the experimental process (Júnior et al., 2019).

As shown in Fig. 6, we can see that both EDCO and SCIU have excellent performance for the accuracy of unknown source model recognition, while EDCO_B is slightly inferior. The CCF_B method has the lowest accuracy of 89.8% on the UACC, and the CCF_A method is slightly better, with an accuracy of 92.6%. As shown in Fig. 7, we find that the EDCO method proposed in this paper has the best OACC performance at 96.2%, followed by EDCO_B, SCIU, and CCF_A, and the CCF_B method has the worst performance. According to the experimental results shown in Table 2, compared with other methods, EDCO shows great improvement in the recognition rate of known source camera models because EDCO includes more detailed hypersurface envelope characterization of the known class samples. The experimental results of EDCO_B and CCF_B are worse than those of EDCO and CCF_A, respectively, providing additional evidence for the effectiveness of Algorithm 1.

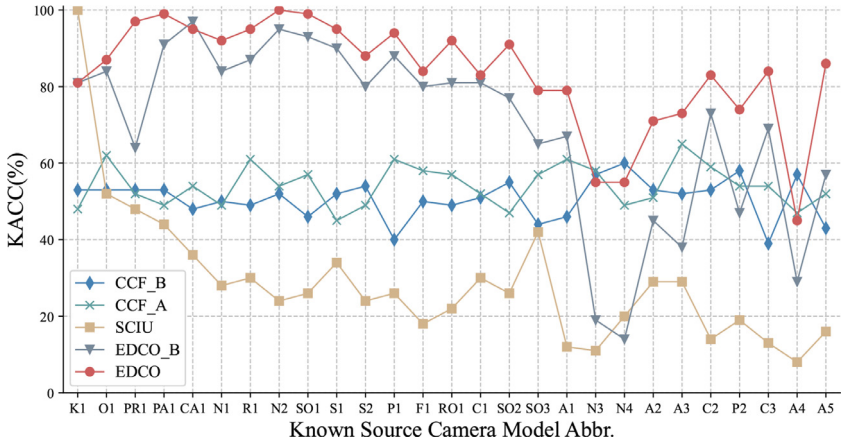

Fig. 5. The known camera model accuracy (%) when there is only one known camera model in the training set.

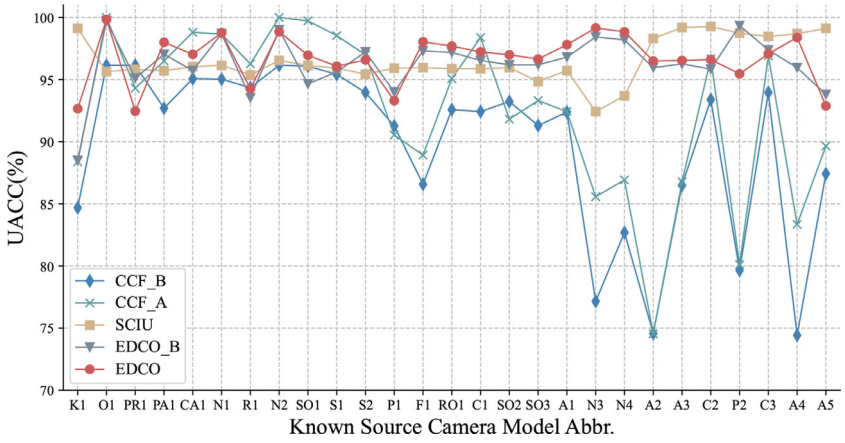

Fig. 6. Unknown camera model accuracy (%) when there is only one known camera model in the training set.

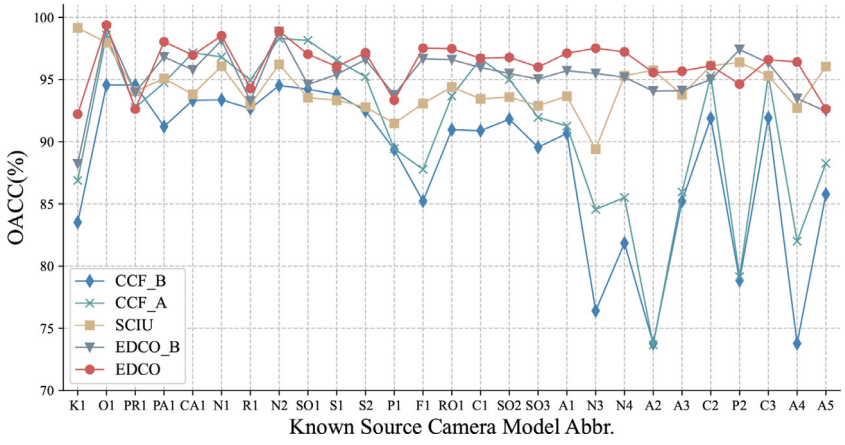

Fig. 7. Overall camera model accuracy (%) when there is only one known camera model in the training set.

Experiment II: To compare the approach adapted from Mayer et al. similarity Mayer et al. (2020); Mayer and Stamm (2018), we assessed the performance of our proposed EDCO method for determining whether two images are captured by different or the same camera models.

Fig. 8 shows the rates of correctly detecting two images as sourced from different camera models:

1. **Known vs Known**: both images captured by the camera models known to the test model.
2. **Known vs Unknown**: one image captured by a known source camera model and the other by an unknown source camera model.

From the experimental results, we can find that the Mayer et al. similarity method can achieve high accuracy for some image pairs, including O1 and PR1, O1 and PA1,P1 and N2, etc. However, for some image pairs, the Mayer et al. similarity method has low recognition accuracy, for example, only 47.0% accuracy between O1 and S1. Overall, the average accuracy of the EDCO method is the better than the Mayer et al. similarity method. However, in

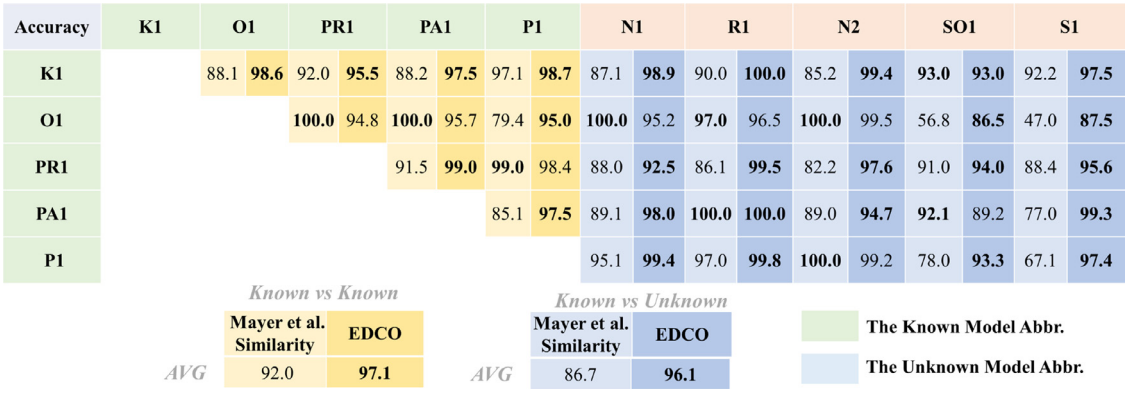

Fig. 8. Overall accuracy (%) performance comparison: Mayer et al. similarity and EDCO.

Table 3
Overall accuracy (%) on the VISION dataset.

KNOWN MODEL	KACC	UACC	OACC
Samsung_GalaxyS3Mini	85.0	99.7	98.3
Apple_iPhone4s	90.0	93.9	93.5
Huawei_P9	77.5	98.9	96.8
LG_D290	82.5	99.7	98.0
Lenovo_P70A	72.5	98.6	96.0
Sony_XperiaZ1Compact	87.5	94.4	93.8
Microsoft_Lumia640LTE	90.0	88.1	88.3
OnePlus_A3000	75.0	97.8	95.5
Samsung_GalaxyS5	100.0	100.0	100.0
Huawei_P8	95.0	90.6	91.0
AVERAGE	**85.5**	**96.1**	**95.1**

Table 4
Overall accuracy (%) on the Kaggle dataset.

KNOWN MODEL	KACC	UACC	OACC
HTC_1_M7	78.0	90.8	89.5
iPhone_4s	89.0	89.3	89.3
iPhone_6	80.5	95.0	93.5
LG_Nexus_5x	90.2	88.3	88.5
Droid_Maxx	62.2	94.2	91.0
Moto_Nexus_6	62.2	97.7	94.1
Moto_X	65.9	82.1	80.5
Galaxy_Note3	70.7	99.6	96.7
Galaxy_S4	36.6	100.0	93.7
Sony_NEX_7	91.5	100.0	99.1
AVERAGE	**72.7**	**93.7**	**91.6**

terms of the recognition accuracy of some image pairs, the Mayer et al. similarity method achieves the highest recognition accuracy of 100% (6 times), followed by EDCO (2 times).

Experiment III: In order to prove the universality of the EDCO method proposed in this paper, additional experiment is carried out on the VISION dataset (Shullani et al., 2017), which contains more than 35,000 images and videos captured using 35 different portable devices of 11 major brands. We select 200 high-quality images from each of the 10 brands and set them into training sets and verification sets at a ratio of 7:3. According to the data shown in Table 3, it can be seen that the EDCO method proposed in this paper still achieves a good effect on the Vision dataset, in which the average accuracy of KACC, UACC and OACC are marked in bold font.

In addition, we test the proposed method EDCO on the dataset of IEEE's Signal Processing Society-camera Model Identification Kaggle Competition (Stamm et al., 2018). The Kaggle dataset constitutes of 275 images each from 10 different smartphone camera models, including point-and-shoot cameras, cell phone cameras, and digital single-lens reflex cameras. All images are captured and stored as JPEGs using the default settings. The Kaggle dataset is divided into training set and verification set in a ratio of 7:3 for experiments. According to the data shown in Table 4, it can be seen that the EDCO method proposed in this paper still achieves a good effect on the Kaggle dataset.

4.3.2. Ablation study

As discussed above, the EDCO method shows some significant advancements toward source camera identification on the open set when the experimental conditions are extremely harsh (there is only one class of camera models from known sources and 26 classes of camera models from unknown sources). In this section, we will compare the other distributions of the dataset and make a systematic comparison with the recent state-of-the-art methods.

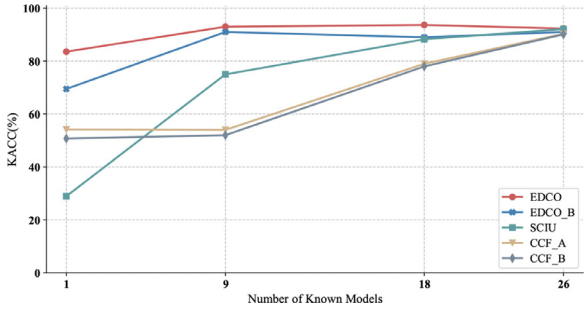

Fig. 9. Known camera model accuracy (%) values for the compared methods.

As shown in Fig. 9, with the increase in the number of known camera models, the KACC values increase for all the methods. When the number of known models in the training set is first increased, the performance of the SCIU method is greatly improved. Moreover, since CCF_A and CCF_B need more known source camera models for training, their KACC values improve relatively slowly with the increase in the number of known models. The EDCO and EDCO_B methods are relatively robustm and EDCO is superior to other methods in both average accuracy and method stability.

An examination of the experimental results presented in Fig. 10 shows that the UACC values for all methods decrease with an increasing number of known source camera models; the reason is that the training set has more positive class samples with an increase in the number of known models and sample size, so the description of the boundary of the positive class samples is more abundant. At the same time, the number of samples from unknown sources decreases, and the proportion of errors from unknown camera models in the total number of samples from unknown sources increases.

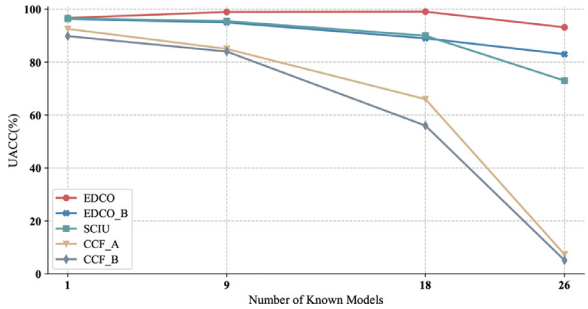

Fig. 10. Unknown camera model accuracy (%) values for the compared methods.

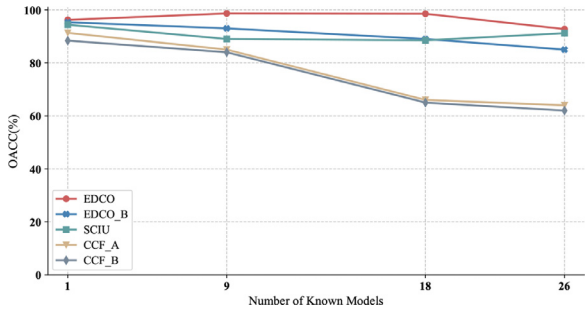

Fig. 11. Overall camera model accuracy (%) values of the compared methods.

In Fig. 11, we can see that with the increase in the number of camera models from known sources, both the EDCO and SCIU methods are stable in terms of OACC, but the overall recognition accuracy of the proposed EDCO method is slightly higher.

5. Conclusion

In this paper, we propose a novel EDCO method for camera model identification on the open set. That is, given an image captured by camera models that are unknown for the existing classifier, EDCO is able to efficiently and effective identify the image. Furthermore, EDCO can update the classifier with a new-found model without retraining with the whole dataset and then link the input images to the corresponding class with high accuracy, as demonstrated by our experiments.

Future work will focus on two directions. First, the source of the unknown samples that have been separated can be further classified; however, this requires intense efforts because the number of specific categories of the unknown source camera models is unknown. Second, the flexibility of the algorithm can be further improved through data-adaptive processing.

Declaration of Competing Interest

The authors declare that they have no known competing financial interests or personal relationships that could have appeared to influence the work reported in this paper.

CRediT authorship contribution statement

Bo Wang: Conceptualization, Supervision, Project administration. **Yue Wang:** Data curation, Writing – original draft, Methodology, Software. **Jiayao Hou:** Visualization, Investigation, Validation. **Yi Li:** Writing – review & editing. **Yanqing Guo:** Writing – review & editing.

Acknowledgment

This work is supported by the National Natural Science Foundation of China (No. U1936117, No. 62076052, No. 61772111), the Science and Technology Innovation Foundation of Dalian (No. 2021JJ12GX018), and the Fundamental Research Funds for the Central Universities (DUT21GF303, DUT20TD110, DUT20RC(3)088).

Supplementary materials

Supplementary material associated with this article can be found, in the online version, at doi:10.1016/j.ejps.2020.105216.

References

Ahmed, F., Khelifi, F., Lawgaly, A., Bouridane, A., 2019. Comparative analysis of a deep convolutional neural network for source camera identification. In: 2019 IEEE 12th International Conference on Global Security, Safety and Sustainability, pp. 1–6.

Alattar, A.M., Memon, N.D., Heitzenrater, C.D., Goljan, M., Fridrich, J., 2015. Cfa-aware features for steganalysis of color images. In: Proceedings of SPIE - The International Society for Optical Engineering, 9409. 94090V–94090V–13

Bayar, B., Stamm, M., 2017. Design principles of convolutional neural networks for multimedia forensics. Electronic Imaging 2017 (7), 77–86.

Bayar, B., Stamm, M., 2018. Towards open set camera model identification using a deep learning framework. In: IEEE International Conference on Acoustics, Speech and Signal Processing, pp. 2007–2011.

Bayram, S., Sencar, H., Memon, N., Avcibas, I., 2005. Source camera identification based on CFA interpolation. In: IEEE International Conference on Image Processing, 3, pp. III–69.

Bondi, L., Baroffio, L., Guera, D., Bestagini, P., Delp, E., Tubaro, S., 2017a. First steps toward camera model identification with convolutional neural networks. IEEE Signal Process Lett 24, 259–263.

Bondi, L., Güera, D., Baroffio, L., Bestagini, P., Delp, E., Tubaro, S., 2017b. A preliminary study on convolutional neural networks for camera model identification. In: Media Watermarking, Security, and Forensics, pp. 67–76.

Choi, K., Lam, E., Wong, K., 2006. Automatic source camera identification using the intrinsic lens radial distortion. Opt Express 14 (24), 11551–11565.

Costa, F.O., Eckmann, M., Scheirer, W., Rocha, A., 2012. Open set source camera attribution. In: 2012 25th SIBGRAPI Conference on Graphics, Patterns and Images, pp. 71–78.

Costa, F.O., Silva, E., Eckmann, M., Scheirer, W., Rocha, A., 2014. Open set source camera attribution and device linking. Pattern Recognit Lett 39, 92–101.

Freire-Obregón, D., Narducci, F., Barra, S., Castrillón-Santana, M., 2019. Deep learning for source camera identification on mobile devices. Pattern Recognit Lett 126, 86–91.

Gao, S., Xu, G., Hu, R.M., 2012. Camera model identification based on the characteristic of CFA and interpolation. In: Shi, Y.Q., Kim, H.J., Perez-Gonzalez, F. (Eds.), Digital Forensics and Watermarking. Springer Berlin Heidelberg, Berlin, Heidelberg, pp. 268–280.

García, J., Crawford, B., Soto, R., Castro, C., Paredes, F., 2018. A k-means binarization framework applied to multidimensional knapsack problem. Applied Intelligence 48 (13), 357–380.

Gloe, T., Böhme, R., 2010. The dresden image database for benchmarking digital image forensics, volume 3, pp. 1584–1590. doi:10.1080/15567281.2010.531500.

González, R., Woods, R., 1981. Digital image processing. IEEE Trans Pattern Anal Mach Intell PAMI-3, 242–243.

Huang, Y., Cao, L., Zhang, J., Pan, L., Liu, Y., 2018. Exploring feature coupling and model coupling for image source identification. IEEE Trans. Inf. Forensics Secur. 13 (12), 3108–3121.

Huang, Y., Zhang, J., Huang, H., 2015. Camera model identification with unknown models. IEEE Trans. Inf. Forensics Secur. 10, 2692–2704.

Júnior, P.R.M., Bondi, L., Bestagini, P., Tubaro, S., Rocha, A., 2019. An in-depth study on open-set camera model identification. IEEE Access 7, 180713–180726.

Kang, X., Li, Y., Qu, Z., Huang, J., 2012. Enhancing source camera identification performance with a camera reference phase sensor pattern noise. Information Forensics and Security, IEEE Transactions on 7 (2), 393–402.

Kharrazi, M., Sencar, H.T., Memon, N., 2004. Blind source camera identification. In: 2004 International Conference on Image Processing, 2004. ICIP '04., volume 1, pp. 709–712Vol. 1. doi:10.1109/ICIP.2004.1418853.

Lekshmi, K., Vaithiyanathan, V., 2018. Source camera identification of image for forensic analysis using sensor fingerprints. In: 2018 Fourth International Conference on Computing Communication Control and Automation, pp. 1–5.

Li, C., 2010. Source camera identification using enhanced sensor pattern noise. IEEE Trans Inf Forensics Secur 5, 280–287.

Li, R., Li, C.T., Guan, Y., 2018. Inference of a compact representation of sensor fingerprint for source camera identification. Pattern Recognit 74, 556–567.

Liu, B., Xiao, Y., Cao, L., Hao, Z., Deng, F., 2012. Svdd-based outlier detection on uncertain data. Knowl Inf Syst 34, 597–618.

Liu, L., Zhao, Y., Ni, R., Tian, Q., 2018. Copy-move forgery localization using convolutional neural networks and CFA features. Int J Digit Crime Forensics 10, 140–155.
Liu, Y., Huang, Y., Zhang, J., Shen, H., 2019. Anti-noise image source identification. Concurrency and Computation: Practice and Experience 31 (19).
Mayer, O., Hosler, B.C., Stamm, M., 2020. Open set video camera model verification. In: ICASSP 2020 - 2020 IEEE International Conference on Acoustics, Speech and Signal Processing, pp. 2962–2966.
Mayer, O., Stamm, M., 2018. Learned forensic source similarity for unknown camera models. In: IEEE International Conference on Acoustics, Speech and Signal Processing, pp. 2012–2016.
Rafi, A.M., Wu, J., Hasan, M.K., 2020. L2-constrained remnet for camera model identification and image manipulation detection, volume 12538 LNCS, pp. 267–282.
Sameer, V.U., Naskar, R., 2020. Deep siamese network for limited labels classification in source camera identification. Multimed Tools Appl 79 (37–38), 28079–28104.
Schweighofer, G., Segvic, S., Pinz, A., 2008. Online/realtime structure and motion for general camera models. In: 2008 IEEE Workshop on Applications of Computer Vision, pp. 1–6.
Shullani, D., Fontani, M., Iuliani, M., Shaya, O.A., Piva, A., 2017. Vision: a video and image dataset for source identification. EURASIP Journal on Information Security 2017 (1), 15. doi:10.1186/s13635-017-0067-2.
Stamm, M., Bestagini, P., Marcenaro, L., Campisi, P., 2018. Forensic camera model identification: highlights from the IEEE signal processing cup 2018 student competition [SP competitions]. IEEE Signal Process Mag 35 (5), 168–174.
Tax, D., Duin, R.P., 2004. Support vector data description. Mach Learn 54, 45–66.
Tuama, A., Comby, F., Chaumont, M., 2016. Camera model identification with the use of deep convolutional neural networks. In: IEEE International Workshop on Information Forensics and Security, pp. 1–6.
Wang, B., Kong, X., You, X., 2009. Source camera identification using support vector machines. Advances in Digital Forensics V.
Wang, B., Zhong, K., Li, M., 2018. Ensemble classifier based source camera identification using fusion features. Multimed Tools Appl 78, 8397–8422.
Xu, G., Shi, Y., 2012. Camera model identification using local binary patterns. In: 2012 IEEE International Conference on Multimedia and Expo, pp. 392–397.
Yang, P., Ni, R., Zhao, Y., Zhao, W., 2019. Source camera identification based on content-adaptive fusion residual networks. Pattern Recognit Lett 119, 195–204.
Zheng, Y., Cao, Y., Chang, C., 2020. A PUF-based data-device hash for tampered image detection and source camera identification. IEEE Trans. Inf. Forensics Secur. 15, 620–634.

Bo Wang received his B.S. degree in electronic and information engineering and his M.S. degree and Ph.D. degree in signal and information processing from Dalian University of Technology, Dalian, China, in 2003, 2005 and 2010, respectively. From 2010 to 2012, he was a postdoctoral research associate with the faculty of Management and Economics at Dalian University of Technology. He is currently an associate professor in the School of Information and Communication Engineering at Dalian University of Technology. His current research interests focus on the areas of multimedia processing and security and artificial intelligence security.

Yue Wang received her B.S. degree in Communication Engineering from Shenyang University of Technology, China, in 2019. She is currently pursuing her M.S. degree in Electronic and Communication Engineering from Dalian University of Technology, Dalian, China. Her current research interests are image processing and digital image forensics.

Jiayao Hou received his B.S. degree in Electronic and Information Engineering from Dalian University of Technology, China, in 2020. He is currently pursuing his M.S. degree in Electronic and Communication Engineering from Dalian University of Technology, Dalian, China. His current research interests are image processing and digital image forensics.

Yi Li received the B.E. and M.E. degrees from the Dalian University of Technology (DUT), Dalian, China, in 2014 and 2017, respectively, and the Ph.D. degree from the University of Chinese Academy of Sciences (UCAS), Beijing, China, in 2020. She is currently an Associate Professor with the School of Artificial Intelligence, DUT. Her research interests include computer vision, pattern recognition and multimedia computing.

Yanqing Guo is with the School of Information and Communication Engineering, Dalian University of Technology, Dalian, China. Yanqing Guo (M' 13) received his B.S. and Ph.D. degrees in electronic engineering from the Dalian University of Technology of China, Dalian, China, in 2002 and 2009, respectively. He is currently a Professor with the Faculty of Electronic Information and Electrical Engineering, Dalian University of Technology. His research interests include machine learning, computer vision, and multimedia security.